THE JOURNAL OF PHYSICAL CHEMISTRY Letters

Cite This: J. Phys. Chem. Lett. 2019, 10, 4788−4793

Letter

pubs.acs.org/JPCL

Light-Assisted Diazonium Functionalization of Graphene and Spatial Heterogeneities in Reactivity

Yunqi Li,[†] Wan Li,[†] Michal Wojcik,[†] Bowen Wang,[†] Liang-Chun Lin,[§] Markus B. Raschke,[§] and Ke Xu*[,†,‡]

[†]Department of Chemistry, University of California, Berkeley, California 94720, United States

[§]Department of Physics, Department of Chemistry, and JILA, University of Colorado, Boulder, Colorado 80309, United States

[‡]Division of Molecular Biophysics and Integrated Bioimaging, Lawrence Berkeley National Laboratory, Berkeley, California 94720, United States

Supporting Information

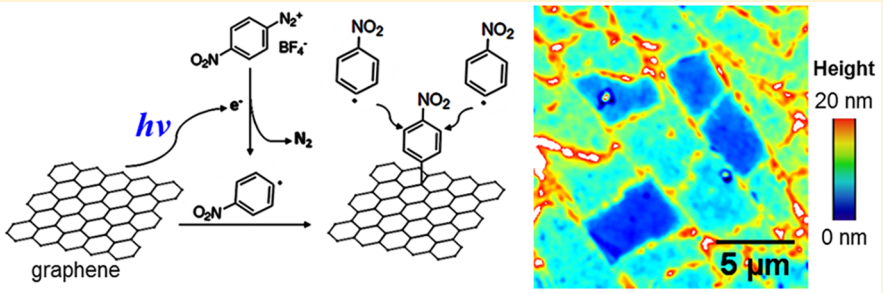

ABSTRACT: The reaction of monolayer graphene with aryl diazonium salts is a popular approach for functionalizing graphene under ambient conditions. We here apply interference reflection microscopy (IRM), a label-free optical technique, to study the in situ reaction dynamics of the representative diazonium reaction of graphene with 4-nitrobenzenediazonium tetrafluoroborate (4-NBD) at high spatiotemporal resolution and further correlate results with atomic force microscopy, Raman spectroscopy, and infrared scattering scanning near-field optical microscopy. Interestingly, we find the reaction to be significantly promoted by a low (0.5 W/cm^2) level of blue visible light, whereas at the same intensity level, red light has negligible effects on reaction rate. We further report rich spatial heterogeneities for the reaction, including enhanced reactivity at graphene edges and an unexpected flake-to-flake variation in reaction rate. Moreover, we demonstrate direct photopatterning for the 4-NBD functionalization, achieving 400 nm patterning resolution.

The promise of graphene, a key two-dimensional material with outstanding optical, electrical, and mechanical properties,[1,2] is substantially expanded through chemistry, from the tuning of electronic properties to the addition of different functionalities toward applications.[3−6] To overcome the low chemical reactivity of the graphene basal plane, reaction with the highly reactive radicals produced from aryl diazonium salts has been one of the most common approaches for the functionalization of graphene under ambient conditions.[7−16] However, it has been difficult to monitor the reaction dynamics of this important system, given that graphene is only a single layer of carbon atoms. We recently developed a facile, label-free approach based on interference reflection microscopy (IRM) to record in situ the mechanical properties[17] and reaction dynamics[18,19] of graphene with ∼300 nm spatial resolution and video-rate temporal resolution. In particular, for the oxidation of graphene, we have visualized rich spatiotemporal heterogeneities and demonstrated how it could be driven reversibly through electrochemistry.[18,19]

Here we apply IRM to study the prototype diazonium reaction of graphene with 4-nitrobenzenediazonium tetrafluoroborate (4-NBD).[7−10,12−16] Unexpectedly, we find a light-driven mechanism that is highly effective at low light intensities. The reaction is sensitive to the illumination wavelength, so that at the same intensity level, blue visible light strongly promotes the reaction, whereas red light has no apparent effects when compared to the dark reaction. Moreover, we report rich spatial heterogeneity for the reaction, including substantially faster reactions at graphene edges and an unexpected flake-to-flake variation in reaction rate. Finally, we demonstrate the direct photopatterning of 4-NBD functionalization, achieving ∼400 nm patterning resolution.

Copper-grown monolayer graphene[20] was transferred onto a glass coverslip substrate, which was then mounted onto an IRM system based on a wide-field inverted microscope.[17,18] The sample was immersed under an aqueous solution of 4 mg/mL (16.9 mM) 4-NBD. The illumination light entered from the bottom through the glass substrate as a near-parallel beam

Received: July 30, 2019
Accepted: August 5, 2019
Published: August 5, 2019

DOI: 10.1021/acs.jpclett.9b02225
J. Phys. Chem. Lett. 2019, 10, 4788−4793

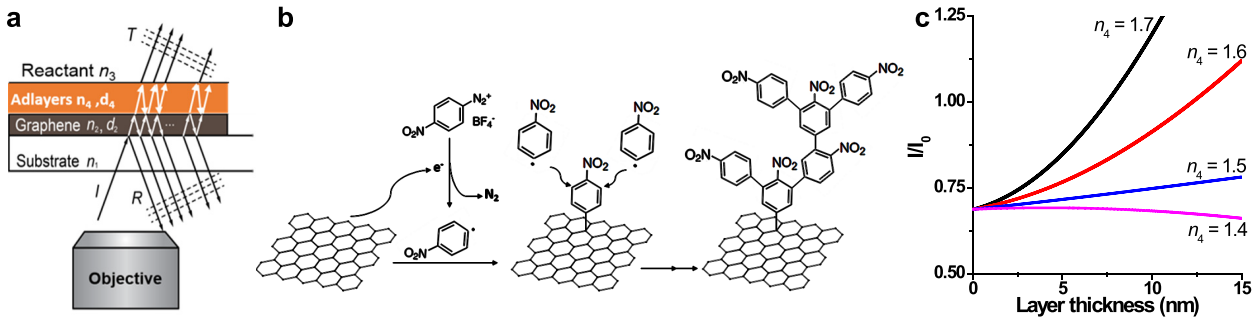

Figure 1. IRM visualization of the diazonium functionalization of graphene. (a) Schematic of the system. n_1, n_2, n_3, and n_4 denote the complex indices of refraction for the substrate, graphene, the reactant solution, and the functionalized layer on top of graphene, respectively. (b) Reaction scheme for the reaction of graphene with 4-NBD. (c) The predicted IRM signal at 450 nm wavelength for monolayer graphene as a function of the thickness of the functionalized layer, for layers of different refractive indices n_4.

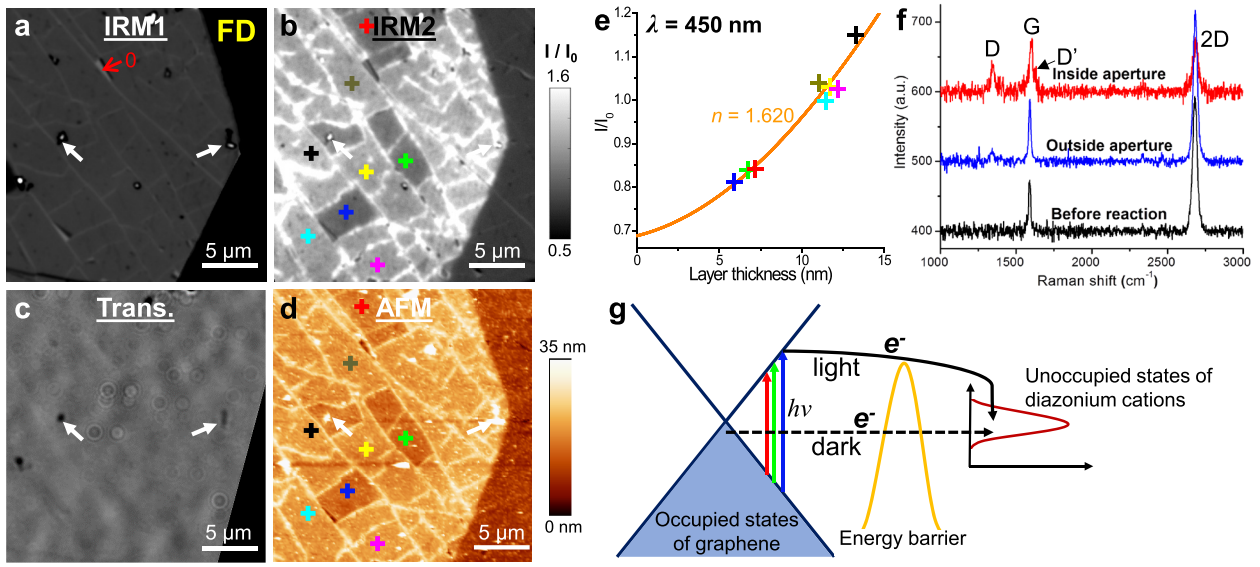

Figure 2. IRM reveals a strong light dependence of the diazonium reaction. (a and b) IRM images of monolayer graphene, before (a) and after (b) 220 s of reaction in the 4-NBD solution under continuous illumination of 0.5 W/cm^2 at 450 nm. Note that in panel a, a field diaphragm aperture (marked as "FD" in the image) confined the illumination area, whereas in panel b, this confinement was removed to image the full view. "0" points to exposed glass surface due to a local tear in graphene. (c and d) Transmission light microscopy (c) and AFM (d) images of the same region as panel b after the reaction. White arrows in panels a–d point to debris observed across different microscopy modes, which aided alignment. (e) Local IRM contrast versus the AFM-determined height of the functionalized layer, for different parts of the sample marked by the colored crosses in panels b and d. Orange curve: fit to eq 1, yielding n_4 = 1.620. (f) Raman spectra after the reaction, for regions inside (red line) and outside (blue line) the optical aperture, compared to pristine graphene (black line). (g) A possible hot electron-transfer mechanism for the reaction.

and was reflected and interfered with itself at the graphene sample (Figure 1a).

According to the general mechanism of the diazonium reaction (Figure 1b),[15,21] a delocalized electron is transferred from graphene to the aryl diazonium cation, thus generating an aryl radical after the release of N_2. The aryl radical covalently reacts with the graphene surface but also reacts with the already attached aryl molecules to form a nanometer-thick polymer layer.[13,16,21] Through transfer-matrix analysis based on modifications to our previous model,[17] the presence of a thin dielectric layer on top of monolayer graphene would substantially alter the local IRM signal:

$$I = \left| \frac{e^{i(\phi_2+\phi_4)}r_{12} + e^{-i(\phi_2-\phi_4)}r_{24} + e^{-i(\phi_2+\phi_4)}r_{43} + e^{i(\phi_2-\phi_4)}r_{12}r_{24}r_{43}}{e^{i(\phi_2+\phi_4)} + e^{-i(\phi_2-\phi_4)}r_{12}r_{24} + e^{-i(\phi_2+\phi_4)}r_{12}r_{43} + e^{i(\phi_2-\phi_4)}r_{24}r_{43}} \right|^2 I_I \quad (1)$$

Here I_I is the intensity of the incident light, $r_{12} = (n_1 - n_2)/(n_1 + n_2)$, $r_{24} = (n_2 - n_4)/(n_2 + n_4)$, and $r_{43} = (n_4 - n_3)/(n_4 + n_3)$, with n_1, n_2, n_3, and n_4 being the complex refractive indices of the substrate, graphene, reaction solution, and the functionalized layer, respectively. $\varphi_2 = 2\pi n_2 d_2/\lambda$ and $\varphi_4 = 2\pi n_4 d_4/\lambda$ correspond to phase changes, with d_2 = 0.335 nm and d_4 being the thickness of graphene and the functionalized layer, respectively, and λ being the wavelength of the incident light. Meanwhile, the IRM signal measured at a bare glass substrate (an n_1–n_3 interface) is[17]

$$I_0 = \left| \frac{n_1 - n_3}{n_1 + n_3} \right|^2 I_I \quad (2)$$

Plotting the normalized IRM signal (I/I_0) as predicted by eqs 1 and 2 as a function of d_4 (Figure 1c) suggests monotonic changes in the IRM signal for increased thickness of the functionalized layer, with particularly high sensitivities for $n_4 >$ ~1.6.

We started by monitoring the reaction using 450 nm illumination obtained by applying a 10 nm bandwidth

DOI: 10.1021/acs.jpclett.9b02225
J. Phys. Chem. Lett. 2019, 10, 4788–4793

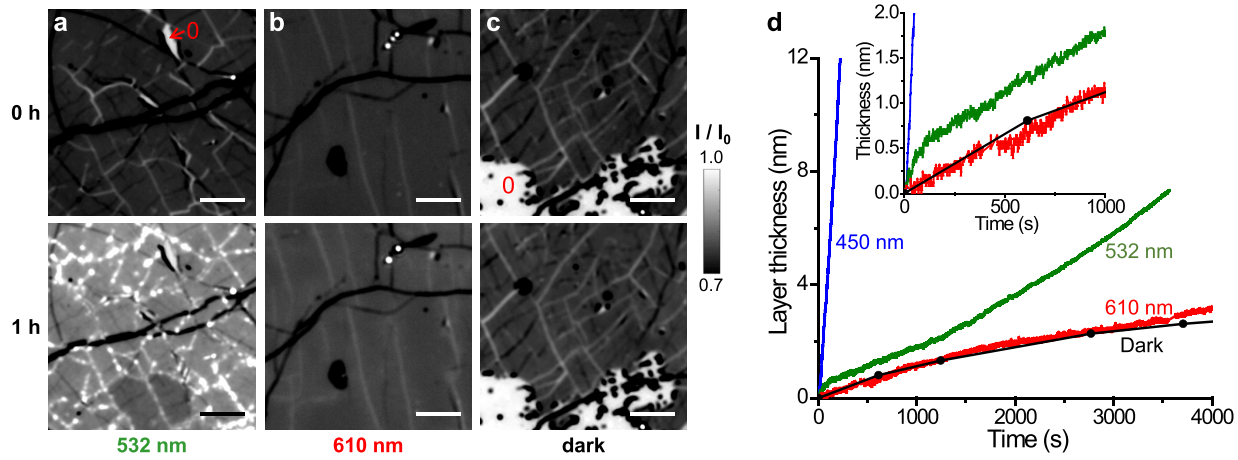

Figure 3. IRM unveils a marked dependence of reaction rate on illumination wavelength. (a–c) IRM images of monolayer graphene before (top panels) and after (bottom panels) 1 h reaction with 4-NBD under 532 nm (a) and 610 nm (b) illumination at 0.6 W/cm^2 and under dark conditions (c). Scale bars: 5 μm. Note that when compared to Figure 2a,b, here a narrower range of I/I_0 is chosen to better present the lower levels of reaction. "0"s in panels a and c mark areas with no graphene coverage. (d) In situ IRM results of layer thickness for typical basal-plane regions for the reaction under 450 nm (blue), 532 nm (green), and 610 nm (red) and in the dark (black). For the "dark" sample, short (~10 s) exposures at 610 nm were intermittently applied to inspect the reaction for just a few time points, whereas continuous illumination was used for the other conditions. Inset: zoomed-in view of the first 1000 s.

bandpass filter on a lamp, thus achieving a relatively low illumination intensity of ~0.5 W/cm^2 in the wide field. A rapid increase in the IRM signal (I/I_0) was observed (Figures 2a,b and S1), suggesting reaction at the graphene surface. Unexpectedly, after 220 s of reaction, we observed a sharp contrast in IRM signal between regions inside and outside the 450 nm illuminated area; hence, a clear boundary was defined by the illumination aperture (field diaphragm) (Figure 2b). Meanwhile, conventional transmission microscopy showed limited contrast (Figure 2c); detailed analysis indicated that graphene absorbed ~2% of the transmitted light,[22] which did not change significantly before and after the reaction.

Raman spectroscopy, carried out after rinsing and air-drying the sample, showed a strong D peak, the appearance of a D′ peak, and a significantly reduced 2D peak for a region inside the illumination aperture (Figure 2f), indicating substantial reaction. In contrast, only a small D peak showed up for regions outside the optical aperture (Figure 2f), consistent with the known low reaction rate of this system at room temperature.[7,9,14] Meanwhile, atomic force microscopy (AFM) showed a ~10 nm height increase for the 450 nm exposed region (Figure 2d); local variations in height were noted, which correlated well with the local IRM signal (Figure 2e). Infrared scattering scanning near-field optical microscopy (*s*-SNOM)[23] further showed that such local variations in layer height correlated well with the strength of the local nitro ($-NO_2$) infrared signal arising from the NO symmetric stretch vibrational mode (Figure S2), consistent with the expected surface polymerization process of 4-NBD (Figure 1b). Whereas we will discuss the local height variations in further detail below, here fitting the IRM signal-AFM height relationship for different parts of the sample to eq 1 (Figure 2e) gave n_4 = 1.620, a value comparable to polymers of related structures (e.g., 1.614 at 450 nm for polystyrene).

Together, our results indicate that the diazonium functionalization of graphene is strongly promoted by 450 nm illumination. The photochemical addition reaction of graphene has been previously examined for peroxides and halogens for its potential controllability and patterning capability.[24−28] In our case, because 4-NBD is transparent over the visible range, similar to the case of benzoyl peroxide (BPO), a similar hot electron-transfer mechanism[24,28] may be invoked, in which the photoexcited graphene transfers a hot electron to the unoccupied states in aryl diazonium cations (Figure 2g) to facilitate the radical generation and subsequent reaction with graphene (Figure 1b). Although the Fermi energy of undoped graphene is comparable to that of the unoccupied states in 4-NBD,[15] the dark reaction is slow at room temperature,[7,9,14] possibly because of an energy barrier that needs to be overcome for the electron-transfer process (Figure 2g), as discussed previously for the BPO system.[28] However, we note that the light intensity in our work (~0.5 W/cm^2) is 5 orders of magnitude lower than previously used for BPO (~10^5 W/cm^2 by focusing a ~1 mW laser into a ~1 μm spot).[24,28] This substantial difference may be related to a higher reactivity of 4-NBD and/or the ease of transferring electrons to diazonium cations in the aqueous solution when compared to BPO in organic solutions. A comparison of the reaction rate and the amount of light absorbed by graphene (~2.3%[22]) gave an apparent quantum yield of ~1 × 10^{-3}, reasonably high for the electron-transfer mechanism.

We next found the reaction kinetics to be highly dependent on the illumination light wavelength. At a comparable intensity level, illumination with a 532 nm green light for 1 h (Figure 3a) led to substantially less reaction when compared to that achieved within 220 s under the 450 nm blue illumination (Figure 2b). Plotting the layer thickness, as converted from the in situ IRM data (Figures S1 and S3), against the reaction time (Figure 3d) showed a ~7-fold difference in reaction rate for the initial reaction, with the reaction rate under the 532 nm illumination further dropping by more than one-half after the first ~0.6 nm. Even lower reactivity was observed for the 610 nm red light (Figures 3b and S4), under which condition the reaction kinetics was similar to that in the dark (Figure 3c,d).

The observed strong dependence on illumination wavelength is consistent with the above hot electron-transfer mechanism (Figure 2g): whereas graphene uniformly absorbs ~2.3% of incident light over the visible spectrum,[22] shorter

DOI: 10.1021/acs.jpclett.9b02225
J. Phys. Chem. Lett. 2019, 10, 4788−4793

wavelengths generate photoexcited electrons of higher energy, which better overcome the reaction barrier. Indeed, previous work on the photochemical reaction of graphene with BPO has found that when compared to the 514 nm illumination, reactions under 458 and 633 nm illuminations are ~5 times faster and ~10 times slower, respectively.[24] Our results followed a similar trend, although the light intensity involved was ~10^5 lower, and that the long-wavelength reaction competed with dark reactions, both effects possibly related to the higher reactivity of 4-NBD.

We next turn to the rich spatial heterogeneity visualized by IRM. One marked feature we found was the brightening-up of IRM signals at graphene edges during the reactions (Figures 2b and 3), indicating a higher local reactivity. Correlated AFM images verified that these higher local IRM signals indeed corresponded to taller local layers (Figure 2d). Examining the in situ IRM data over time (Figures 4 and S1) showed that the reaction rate at the graphene edges are consistently faster than the basal plane throughout the reaction. This result may be interpreted as indicating that the graphene edges contained a higher level of structural defects and so are chemically more reactive.[9,11] Interestingly, our previous IRM work found no reaction enhancement for graphene edges during chemical and electrochemical oxidation processes,[18,19] thus indicating that this difference in edge reactivity is reaction-type dependent.

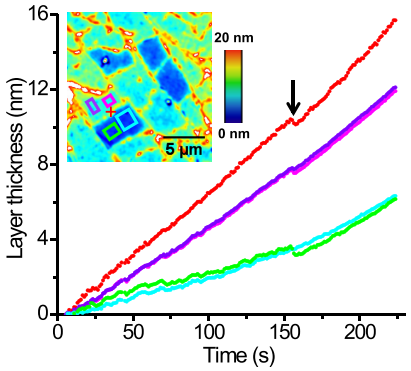

Figure 4. In situ IRM results of the layer thickness as a function of reaction time under 450 nm illumination, for different locations of the same sample. Inset: a color map of layer thickness, for a region shown in Figure 2b. The red curve in the main figure corresponds to a spot at the graphene edge marked by the red cross in the inset, whereas the violet, magenta, green, and cyan curves correspond to four different areas marked by the boxes of corresponding colors in the color map inset. Arrow: artifact due to the adjustment of microscope focus.

Another remarkable IRM observation, corroborated by both AFM and infrared *s*-SNOM results, is an unexpected variation of reactivity between different graphene flakes, even though the reactivity within each continuous flake appeared relatively uniform (Figure 4 and inset). Close examination of the IRM images before reaction (Figure 2a) indicated that these flakes were electrically isolated by nanoscale cracks. Thus, even though they were fragmented from the same initial graphene sheet, they were possibly inadvertently doped to different levels on the glass surface[14] and so shifted to different electrochemical potentials that affected reactivity. For comparison, graphene that contained cracks yet still stayed electrically connected did not exhibit such local variations in reactivity (Figure S5).

Finally, as a possible application for the light-assisted diazonium functionalization discussed above, we examined whether it would be possible to achieve direct photopatterning using this process. To this end, we inserted a photomask into the collimated 488 nm beam path in a home-built wide-field laser microscope,[29] which effectively functioned as a 200× photolithography stepper for samples at the microscope image plane. Thus, exposing a monolayer graphene sample for 120 s under the immersion of a 4-NBD solution led to good photopatterning results, with well-defined fine features down to ~400 nm in size readily obtained (Figures 5 and S6).

In conclusion, through IRM and correlated AFM, Raman, and infrared *s*-SNOM experiments, we have shown that the diazonium functionalization of graphene is significantly promoted by blue light at low levels. Green light was much less effective in promoting the reaction, whereas red light exhibited negligible effects when compared to the dark reaction. While these results are consistent with the hot electron-transfer mechanism previously proposed for the reaction of BPO, the light intensity here for 4-NBD was orders of magnitude lower. We thus demonstrated facile photopatterning in the wide-field at similarly low light intensities, achieving ~400 nm patterning resolution. Together with the rich spatial heterogeneities we further visualized for

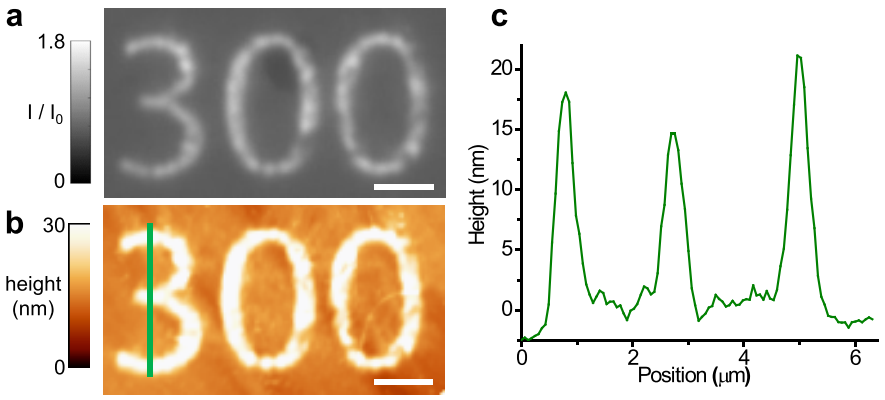

Figure 5. Photopatterning of the graphene surface through light-assisted diazonium reaction. (a) IRM image of a monolayer graphene sample that was exposed with a photomask under 488 nm illumination in a 4-NBD solution, yielding the pattern "300". (b) AFM image of the same region. Scale bars: 2 μm. (c) Height profile along the green line in panel b. Full width at half-maximum (fwhm) of the three peaks were 371, 419, and 408 nm.

DOI: 10.1021/acs.jpclett.9b02225
J. Phys. Chem. Lett. 2019, 10, 4788−4793

the reaction, including enhanced reaction at the edges and the unique flake-to-flake variations in reaction rate, we thus shed new light on one of the most popular approaches for the functionalization of graphene under ambient conditions.

■ ASSOCIATED CONTENT

Supporting Information

The Supporting Information is available free of charge on the ACS Publications website at DOI: 10.1021/acs.jpclett.9b02225.

Materials and methods; IRM and AFM images and infrared *s*-SNOM results (Figures S1−S6) (PDF)

■ AUTHOR INFORMATION

Corresponding Author

*E-mail: xuk@berkeley.edu.

ORCID

Wan Li: 0000-0001-5751-3550

Michal Wojcik: 0000-0002-0053-1018

Markus B. Raschke: 0000-0003-2822-851X

Ke Xu: 0000-0002-2788-194X

Notes

The authors declare no competing financial interest.

■ ACKNOWLEDGMENTS

We thank Dr. Jun Nishida for discussion and Dr. Michael Ross (P. Yang Group) for help with Raman experiments. This work was supported by STROBE, a National Science Foundation Science and Technology Center under Grant No. DMR 1548924, and the Bakar Fellows Award. M.W. acknowledges support from the NSF Graduate Research Fellowship under DGE 1106400. Work at the Molecular Foundry was supported by the U.S. Department of Energy under Contract No. DE-AC02-05CH11231.

■ REFERENCES

(1) Geim, A. K.; Novoselov, K. S. The rise of graphene. *Nat. Mater.* **2007**, *6*, 183−191.

(2) Novoselov, K. S.; Fal'ko, V. I.; Colombo, L.; Gellert, P. R.; Schwab, M. G.; Kim, K. A roadmap for graphene. *Nature* **2012**, *490*, 192−200.

(3) Georgakilas, V.; Otyepka, M.; Bourlinos, A. B.; Chandra, V.; Kim, N.; Kemp, K. C.; Hobza, P.; Zboril, R.; Kim, K. S. Functionalization of graphene: covalent and non-covalent approaches, derivatives and applications. *Chem. Rev.* **2012**, *112*, 6156−6214.

(4) Chua, C. K.; Pumera, M. Covalent chemistry on graphene. *Chem. Soc. Rev.* **2013**, *42*, 3222−3233.

(5) Criado, A.; Melchionna, M.; Marchesan, S.; Prato, M. The covalent functionalization of graphene on substrates. *Angew. Chem., Int. Ed.* **2015**, *54*, 10734−10750.

(6) Kaplan, A.; Yuan, Z.; Benck, J. D.; Rajan, A. G.; Chu, X. S.; Wang, Q. H.; Strano, M. S. Current and future directions in electron transfer chemistry of graphene. *Chem. Soc. Rev.* **2017**, *46*, 4530−4571.

(7) Lomeda, J. R.; Doyle, C. D.; Kosynkin, D. V.; Hwang, W. F.; Tour, J. M. Diazonium functionalization of surfactant-wrapped chemically converted graphene sheets. *J. Am. Chem. Soc.* **2008**, *130*, 16201−16206.

(8) Bekyarova, E.; Itkis, M. E.; Ramesh, P.; Berger, C.; Sprinkle, M.; de Heer, W. A.; Haddon, R. C. Chemical modification of epitaxial graphene: spontaneous grafting of aryl groups. *J. Am. Chem. Soc.* **2009**, *131*, 1336−1337.

(9) Sharma, R.; Baik, J. H.; Perera, C. J.; Strano, M. S. Anomalously large reactivity of single graphene layers and edges toward electron transfer chemistries. *Nano Lett.* **2010**, *10*, 398−405.

(10) Koehler, F. M.; Jacobsen, A.; Ensslin, K.; Stampfer, C.; Stark, W. J. Selective chemical modification of graphene surfaces: distinction between single- and bilayer graphene. *Small* **2010**, *6*, 1125−1130.

(11) Lim, H.; Lee, J. S.; Shin, H. J.; Shin, H. S.; Choi, H. C. Spatially resolved spontaneous reactivity of diazonium salt on edge and basal plane of graphene without surfactant and its doping effect. *Langmuir* **2010**, *26*, 12278−12284.

(12) Niyogi, S.; Bekyarova, E.; Itkis, M. E.; Zhang, H.; Shepperd, K.; Hicks, J.; Sprinkle, M.; Berger, C.; Lau, C. N.; deHeer, W. A.; Conrad, E. H.; Haddon, R. C. Spectroscopy of covalently functionalized graphene. *Nano Lett.* **2010**, *10*, 4061−4066.

(13) Hossain, M. Z.; Walsh, M. A.; Hersam, M. C. Scanning tunneling microscopy, spectroscopy, and nanolithography of epitaxial graphene chemically modified with aryl moieties. *J. Am. Chem. Soc.* **2010**, *132*, 15399−15403.

(14) Wang, Q. H.; Jin, Z.; Kim, K. K.; Hilmer, A. J.; Paulus, G. L. C.; Shih, C. J.; Ham, M. H.; Sanchez-Yamagishi, J. D.; Watanabe, K.; Taniguchi, T.; Kong, J.; Jarillo-Herrero, P.; Strano, M. S. Understanding and controlling the substrate effect on graphene electron-transfer chemistry via reactivity imprint lithography. *Nat. Chem.* **2012**, *4*, 724−732.

(15) Paulus, G. L. C.; Wang, Q. H.; Strano, M. S. Covalent electron transfer chemistry of graphene with diazonium salts. *Acc. Chem. Res.* **2013**, *46*, 160−170.

(16) Greenwood, J.; Phan, T. H.; Fujita, Y.; Li, Z.; Ivasenko, O.; Vanderlinden, W.; Van Gorp, H.; Frederickx, W.; Lu, G.; Tahara, K.; Tobe, Y.; Uji-i, I. H.; Mertens, S. F.; De Feyter, S. Covalent modification of graphene and graphite using diazonium chemistry: tunable grafting and nanomanipulation. *ACS Nano* **2015**, *9*, 5520−5535.

(17) Li, W.; Moon, S.; Wojcik, M.; Xu, K. Direct optical visualization of graphene and its nanoscale defects on transparent substrates. *Nano Lett.* **2016**, *16*, 5027−5031.

(18) Wojcik, M.; Li, Y.; Li, W.; Xu, K. Spatially resolved *in situ* reaction dynamics of graphene via optical microscopy. *J. Am. Chem. Soc.* **2017**, *139*, 5836−5841.

(19) Li, W.; Wojcik, M.; Xu, K. Optical microscopy unveils rapid, reversible electrochemical oxidation and reduction of graphene. *Nano Lett.* **2019**, *19*, 983−989.

(20) Li, X. S.; Cai, W. W.; An, J. H.; Kim, S.; Nah, J.; Yang, D. X.; Piner, R.; Velamakanni, A.; Jung, I.; Tutuc, E.; Banerjee, S. K.; Colombo, L.; Ruoff, R. S. Large-area synthesis of high-quality and uniform graphene films on copper foils. *Science* **2009**, *324*, 1312−1314.

(21) Pinson, J.; Podvorica, F. Attachment of organic layers to conductive or semiconductive surfaces by reduction of diazonium salts. *Chem. Soc. Rev.* **2005**, *34*, 429−439.

(22) Nair, R. R.; Blake, P.; Grigorenko, A. N.; Novoselov, K. S.; Booth, T. J.; Stauber, T.; Peres, N. M. R.; Geim, A. K. Fine structure constant defines visual transparency of graphene. *Science* **2008**, *320*, 1308.

(23) Atkin, J. M.; Berweger, S.; Jones, A. C.; Raschke, M. B. Nano-optical imaging and spectroscopy of order, phases, and domains in complex solids. *Adv. Phys.* **2012**, *61*, 745−842.

(24) Liu, H.; Ryu, S.; Chen, Z.; Steigerwald, M. L.; Nuckolls, C.; Brus, L. E. Photochemical reactivity of graphene. *J. Am. Chem. Soc.* **2009**, *131*, 17099−17101.

(25) Li, B.; Zhou, L.; Wu, D.; Peng, H. L.; Yan, K.; Zhou, Y.; Liu, Z. F. Photochemical chlorination of graphene. *ACS Nano* **2011**, *5*, 5957−5961.

(26) Zhang, L.; Zhou, L.; Yang, M.; Liu, Z.; Xie, Q.; Peng, H.; Liu, Z. Photo-induced free radical modification of graphene. *Small* **2013**, *9*, 1134−1143.

(27) Liao, L.; Song, Z. H.; Zhou, Y.; Wang, H.; Xie, Q.; Peng, H. L.; Liu, Z. F. Photoinduced methylation of graphene. *Small* **2013**, *9*, 1348−1352.

(28) Liao, L.; Wang, H.; Peng, H.; Yin, J. B.; Koh, A. L.; Chen, Y. L.; Xie, Q.; Peng, H. L.; Liu, Z. F. van Hove singularity enhanced

DOI: 10.1021/acs.jpclett.9b02225
J. Phys. Chem. Lett. 2019, 10, 4788−4793

photochemical reactivity of twisted bilayer graphene. *Nano Lett.* **2015**, *15*, 5585−5589.
(29) Wojcik, M.; Hauser, M.; Li, W.; Moon, S.; Xu, K. Graphene-enabled electron microscopy and correlated super-resolution microscopy of wet cells. *Nat. Commun.* **2015**, *6*, 7384.

DOI: 10.1021/acs.jpclett.9b02225
J. Phys. Chem. Lett. 2019, 10, 4788−4793